Available online at www.sciencedirect.com

ScienceDirect

European Journal of Protistology 50 (2014) 329–344

European Journal of PROTISTOLOGY

www.elsevier.com/locate/ejop

Multivariate morphometric analyses of the predatory ciliate genus *Semispathidium* (Ciliophora: Litostomatea), with description of *S. longiarmatum* nov. spec.

Peter Vďačný[a,*], Marek Slovák[b], Wilhelm Foissner[c]

[a] *Department of Zoology, Faculty of Natural Sciences, Comenius University, Mlynská dolina B-1, SK-842 15 Bratislava, Slovak Republic*
[b] *Institute of Botany, Slovak Academy of Sciences, Dúbravská cesta 9, SK-845 23 Bratislava, Slovak Republic*
[c] *FB Organismal Biology, Faculty of Natural Sciences, Salzburg University, Hellbrunnerstrasse 34, A-5020 Salzburg, Austria*

Received 8 January 2014; received in revised form 5 March 2014; accepted 5 March 2014
Available online 18 March 2014

Abstract

We studied morphometrical variation, species boundaries, and importance of morphometric features for a reliable separation of five African *Semispathidium* taxa. Altogether, 20 features traditionally used in alpha-taxonomy of the predatory genus *Semispathidium* were measured or scored on 85 protargol-impregnated interphase specimens, and were analyzed using hierarchical clustering as well as principal component and canonical discriminant analyses. This multivariate approach confirmed that a population found in Botswanan floodplain soil represents a distinct taxon. The new species is described here as *S. longiarmatum*, using live observation, protargol impregnation, and scanning electron microscopy. *Semispathidium longiarmatum* strongly resembles *S. armatum* and *S. breviarmatum* but it is clearly distinguished from these species by the extrusome pattern. The reliability of *S. longiarmatum* is also strengthened, according to the canonical discriminant analysis, by several quantitative features, viz., the number of ciliary rows, the length:width ratio of the macronucleus, and the number of dikinetids in brush row 1. Moreover, the present study documents the distinctness of all African *Semispathidium* species which can be separated by a combination of both qualitative and quantitative (morphometric) features. Consequently, *Semispathidium* species do not form a continuous complex but fairly discrete clusters in the phenotypic space.

Keywords: Africa; Extrusomes; Numerical taxonomy; Resting cyst; Species discrimination

Introduction

Semispathidium Foissner et al., 2002 belongs to the order Spathidiida Foissner and Foissner, 1988, a diverse group of rapacious ciliates that live mainly in terrestrial and semi-terrestrial environments all around the world (Foissner 1998; Foissner and Xu 2007; Foissner et al. 2002). However, the biodiversity center of *Semispathidium* is very likely tropical Africa, since five out of the seven species known, including *S. longiarmatum* nov. spec. described here, have been recorded only from road puddles and floodplain soils in Botswana, Namibia, and South Africa (Foissner et al. 2002, 2010; Vďačný and Foissner 2013; present study). *Semispathidium lagyniforme* (Kahl, 1930) and *S. pulchrum* Foissner et al., 2010 represent an exception, as they have been reported only

*Corresponding author. Tel.: +421 2 602 96 256; fax: +421 2 602 96 333.
E-mail address: vdacny@fns.uniba.sk (P. Vďačný).

http://dx.doi.org/10.1016/j.ejop.2014.03.003
0932-4739/

from soil and ephemeral road or meadow puddles in Europe (Foissner 1984; Foissner et al. 2010; Kahl 1930).

The diagnostic features of the genus *Semispathidium* include a cylindroidal body with a more or less discoidal oral bulge and anteriorly curved ciliary rows forming a spathidiid pattern (Foissner et al. 2002). In vivo identification is based, especially, on the body and extrusome shape and size as well as on the nuclear pattern. Among these markers, extrusomes often play an indispensable role because they are useful species finders also when other features are highly similar (Foissner and Xu 2007; Vďačný and Foissner 2012). However, extrusomes are very important not only for the alpha-taxonomy of predatory ciliates but also for their life histories since they are used to overwhelm and kill the prey by means of paralytic and proteolytic enzymes (Rosati and Modeo 2003; Lynn 2008). Although *Semispathidium* includes only seven nominal species, their extrusome shape and arrangement are comparatively diverse which very likely reflects different predation strategies (e.g., Foissner et al. 1995, 2002, 2010; Foissner and Xu 2007; Lin et al. 2009; Vďačný and Foissner 2012, 2013).

All *Semispathidium* species have been carefully studied not only in vivo but also in protargol-impregnated specimens (Foissner 1984; Foissner et al. 2002, 2010; Vďačný and Foissner 2013; present study). Indeed, protargol preparations provide a wealth of quantitative data that can be assessed, using multivariate methods. Thus, the availability of detailed morphometric data makes this genus an ideal example for studying species boundaries and the importance of morphometric features.

Multivariate techniques have been comparatively rarely used in ciliate taxonomy. For instance, Foissner and Schubert (1983) applied discriminant analysis to separate *Colpoda aspera* Kahl, 1926 from *C. elliotti* Bradbury and Outka, 1967. Using univariate and multivariate statistical methods, Lynn and Malcolm (1983) investigated morphometric variation of 19 clones from eight species of the genus *Colpoda* Müller, 1773 and Berger and Hatzidimitriou (1978) analyzed morphometric variation in the scuticociliate *Ancistrum mytili* (Quennerstedt, 1867) living in mytilid pelecypods. With aid of principal component analysis, Jones and Gates (1994) studied usefulness of traditional morphological criteria in species separation within the *Euplotes charon* morphotype. Another application of multivariate statistical methods in ciliates was provided by Ginoris et al. (2007). These authors showed that discriminant analysis together with neural networks are potentially alternative tools to identify taxa by computer analysis of their digital images.

Material and Methods

Material collecting and processing

African *Semispathidium* taxa were isolated from samples collected in terrestrial and semi-terrestrial habitats of Botswana, Namibia, and the Republic of South Africa. A detailed description of the sites and the material studied is given in the 'Occurrence and ecology' section of the original descriptions: *S. armatum* and *S. enchelyodontides* in Foissner et al. (2002), *S. breviarmatum* in Vďačný and Foissner (2013), *S. longiarmatum* nov. spec. in the present study, and *S. fraterculum* in Foissner et al. (2010). All soils were air-dried for at least one month at room temperature and stored in plastic bags until investigation. The ciliates were reactivated from resting cysts, using the non-flooded Petri dish method, as described in Vďačný and Foissner (2012). The five species were studied with standard taxonomic methods, as described in the following section.

Taxonomic methods

Semispathidium longiarmatum nov. spec. was investigated by a combination of detailed in vivo observation, protargol impregnation, and scanning electron microscopy (SEM). Live observations were conducted at magnifications of 40–1000× with brightfield and differential interference contrast. Protargol impregnation (protocol A) and preparation for SEM followed protocols described by Foissner (1991) and Vďačný and Foissner (2012). In vivo measurements were made at magnifications of 100–1000× while counts and measurements on protargol-impregnated specimens were performed at a magnification of 1000×. Illustrations of live specimens were based on free-hand sketches and/or micrographs while those of prepared cells were made with a drawing device. The formation of resting cysts was induced by isolating cells on concavity slides containing centrifuged soil eluate. These preparations were placed in a moist chamber to prevent drying and checked every day until mature resting cysts were present. Terminology is according to Foissner and Xu (2007).

Multivariate morphometric analyses

A multivariate approach was used to investigate the morphometrical variation of five African *Semispathidium* species and the value of the morphometric features. Altogether, 20 (16 quantitative and four derived ratios) features traditionally used in the alpha-taxonomy of *Semispathidium* and of spathidiids in general (Foissner and Xu 2007), were measured or scored in 85 protargol-impregnated interphase specimens. The individuals were distributed among the five species as follows: 8 specimens of *S. armatum* (Foissner et al. 2002), 19 of *S. breviarmatum* (Vďačný and Foissner 2013), 19 of *S. longiarmatum* sp. n. (present study), 21 of *S. enchelyodontides* (Foissner et al. 2002), and 18 of *S. fraterculum* (Foissner et al. 2010). All morphometric data were retrieved from our original protocols and were compiled in the supplementary Table S1. European taxa, *S. lagyniforme* and *S. pulchrum*, were excluded from the analyses because there were few specimens available for the former species and the original morphometric data of the latter have been lost.

Table S1 related to this article can be found, in the online version, at http://dx.doi.org/10.1016/j.ejop.2014.03.003.

Since most morphometric features were not normally distributed, the non-parametric Spearman coefficient was chosen to assess the extent of correlation. Since highly correlated pairs of features might distort the multivariate analyses, all quantitative features exceeding the critical value ($r > 0.95$) were excluded (Legendre and Legendre 1998).

Cluster Analyses (CA) were carried out using the computer program SYNTAX 2000 (Podani 2001). The CA included a combination of four different algorithms (average linkage, complete linkage, single linkage, and centroid method) with the Euclidean distance and the Manhattan city block distance as coefficients of distance (Marhold 2011).

Principal Component Analysis (PCA) was computed using the SAS 8.2 software (SAS INSTITUTE 2000). Two sets of PCA were performed. The first set (PCA1) was based on a data matrix containing 16 morphometric features and 85 individuals of five taxa while the second set (PCA2) included 15 features and 46 individuals of three morphologically closely related species (*S. armatum*, *S breviarmatum*, and *S. longiarmatum*) that were not clearly separated by the PCA1. Because the number of the macronuclear nodules was constant in the three-taxa dataset, it was excluded from the PCA2.

Potential distinction among *Semispathidium* taxa was tested by three sets of Canonical Discriminant Analysis (CDA), using the computer program SAS. CDA1 was based on 85 individuals of five *Semispathidium* species and 15 features; CDA2A and CDA2B were based on 27 individuals of two closely related taxa (*S. armatum* and *S. longiarmatum*) and 15 and 14 features, respectively. Because the number of the macronuclear nodules did not vary at least in one of the groups, it was not taken into consideration in any CDA dataset. Additionally, the number of ciliary rows was excluded from CDA2B in order to reveal whether further features can be identified for distinguishing *S. armatum* and *S. longiarmatum*.

Results

Description of *Semispathidium longiarmatum* Foissner & Vďačný nov. spec. (Figs 1–5; Table 1)

Diagnosis: Size about 230 × 40 μm in vivo. Shape narrowly to very narrowly ellipsoidal with slightly to moderately oblique oral bulge. Macronucleus narrowly to very narrowly ellipsoidal and usually slightly curved; one micronucleus. Two types of oral bulge extrusomes: type I very narrowly cuneate, about 9–11 × 1 μm in size, forms a bundle in central bulge area; type II oblong, about 2 × 0.3 μm in size, occupies peripheral bulge area. On average 30 ciliary rows, three anteriorly differentiated into a distinctly heterostichad dorsal brush with longest row 2 occupying about 27% of body length.

Type locality: Soil from the Chobe River floodplain, Kabolebole Peninsula, Botswana, Africa, E17°50′ S25°00′.

Type material: The slide containing the protargol-impregnated holotype specimen (inv. no. 2013/50) has been deposited in the Biologiezentrum of the Oberösterreichische Landesmuseum in Linz (LI), Austria. Three paratype slides (inv. nos. 2013/51–53) have been deposited in the same repository. The holotype (Fig. 1B) and relevant paratype specimens have been marked with black ink circles on the coverslip.

Etymology: The species-group name *longiarmatum* is a composite of the stem of the Latin adjective *long·us*, *-a*, *-um* [m, f, n] (long), the thematic vowel *·i-*, and the Latin adjective *armat·us*, *-a*, *-um* [m, f, n] (armed, armored), referring to the comparatively long extrusomes, a main feature of this species.

Description: Size in vivo 165–300 × 35–50 μm, usually near 230 × 40 μm, as calculated from some in vivo measurements and the morphometric data, adding 15% preparation shrinkage (Table 1). Shape narrowly to very narrowly ellipsoidal with a length:width ratio of 3.6–7.4:1; sometimes rod-shaped (Fig. 4A) or broadly fusiform (Fig. 1B); not flattened laterally. Anterior body end more or less narrowing, slightly to moderately inclined ventrally and more or less vaulted dorsally; posterior body end narrowly to broadly rounded (Figs 1A, B, M, N, 2D; Table 1). Nuclear apparatus usually in second third of cell. Macronucleus narrowly to very narrowly ellipsoidal, often slightly curved, about 53 × 11 μm in protargol preparations; nucleoli numerous, globular, small- to medium-sized, well recognizable both in vivo and after protargol impregnation. Micronucleus near or attached to macronucleus at varying positions, globular to broadly ellipsoidal, 2.5–5 μm across in protargol preparations (Figs 1A, B, M, N, 2D; Table 1). Contractile vacuole in posterior body end, several excretory pores well recognizable in pole area in some protargol-impregnated specimens (Figs 1A, B, M, N, 2D); no contractile vacuole in anterior body half. A fecal mass usually 20–30 μm in diameter, frequently attached to contractile vacuole, composed of food remnants deeply impregnating with protargol (Fig. 1M). Two types of extrusomes scattered throughout cytoplasm and attached to oral bulge: type I very narrowly cuneate, about 9–11 × 1 μm in size, forms a big bundle in central bulge area; type II oblong, about 2 × 0.3 μm in size, occupies periphery of oral bulge; cytoplasmic extrusomes sometimes impregnate with protargol while oral extrusomes do not except for anterior (2–3 μm) portion usually slightly, rarely deeply impregnated (Figs 1A, D, F, I, J, 2A, B, 3A, 4C). Cortex very flexible, distinctly furrowed by ciliary rows (Figs 2C, 5D), contains about three oblique granule rows between each two kineties; granules ordinarily spaced both in somatic and oral bulge cortex, about 0.8 × 0.3 μm in size (Fig. 1G). Cytoplasm colourless, packed with lipid droplets 1–5 μm across, extrusomes, and some vacuoles with crystals very likely coming from ingested hypotrichs (Figs 1A, 2B, D). Swims rather rapidly rotating about main

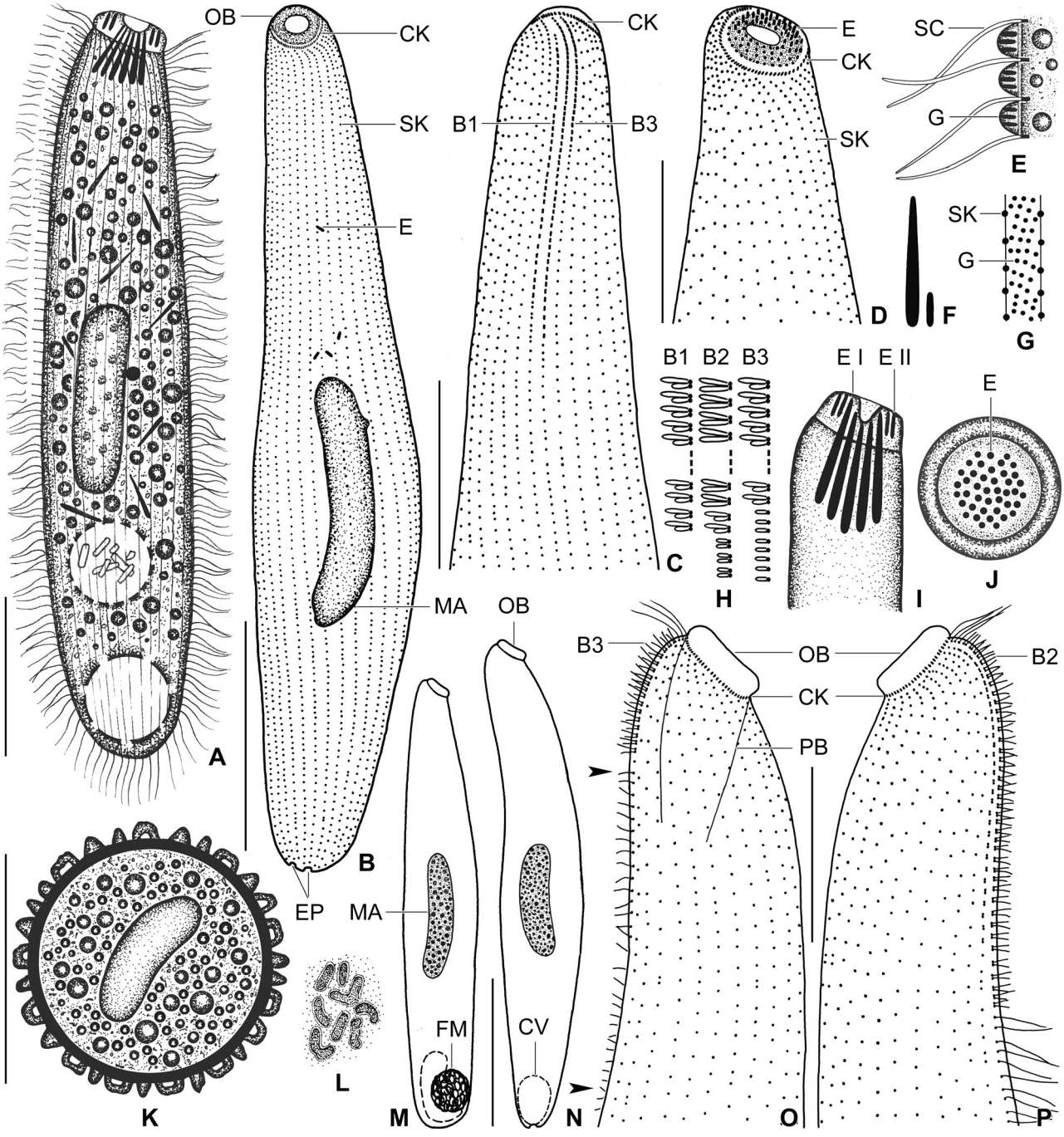

Fig. 1. *Semispathidium longiarmatum* nov. spec. from life (A, E–L) and after protargol impregnation (B–D, M–P). (A) Right side view of a representative specimen, length 230 μm. (B) Ciliary pattern of ventral side and nuclear apparatus of holotype specimen, length 190 μm. (C) Dorsal view of anterior body region of holotype specimen. (D) Ventral view of anterior body region of a paratype specimen. (E, G) Optical section and surface view, showing the cortical granules located in conspicuous alveoli. (F) There are two types of oral bulge extrusomes differing in shape and size. (H) Fine structure of dorsal brush, slightly schematized. (I) Detail of anterior body region, showing the slightly ventrally inclined oral bulge armored with extrusomes. (J) Frontal view, showing the discoidal oral bulge studded with extrusomes. (K) Resting cyst with conspicuous wall. (L) Surface view of resting cyst, showing the small ribs separated by furrows. (M, N) Shape variants. (O, P) Right and left side of anterior body region of a paratype specimen. Arrowheads mark the monokinetidal tail of brush row 3. B1–3, dorsal brush rows; CK, circumoral kinety; CV, contractile vacuole; E(I, II), extrusome types; EP, excretory pores of contractile vacuole; FM, fecal mass; G, cortical granules; MA, macronucleus; OB, oral bulge; PB, pharyngeal basket; SC, somatic cilia; SK, somatic kineties. Scale bars: 20 μm (D, O, P), 30 μm (C), and 50 μm (A, B, K).

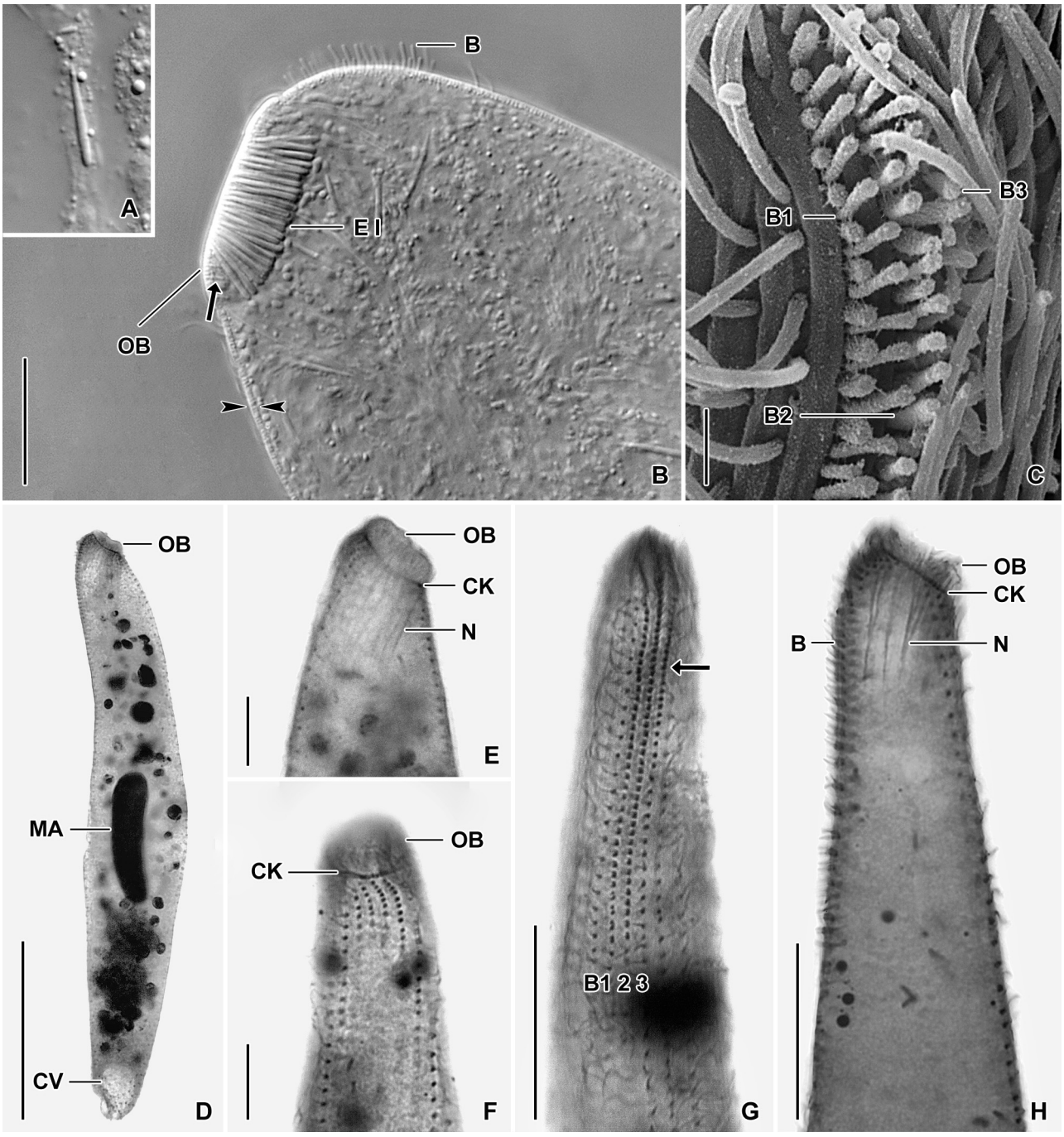

Fig. 2. *Semispathidium longiarmatum* nov. spec. from life (A, B), after protargol impregnation (D–H), and in the SEM (C). (A) The type I extrusomes are very narrowly cuneate and about 9–11 × 1 μm in size. (B) A strongly squeezed specimen, showing the extrusome bundle in the central area of the oral bulge. The arrow denotes a minute type II extrusome. Opposed arrowheads mark cortex. (C) Detail of anterior portion of dorsal brush. The dikinetids of brush row 1 bear a long anterior bristle and a posterior stump while the dikinetids of brush row 2 are associated with bristles of similar length. The cortex is distinctly furrowed by the ciliary rows. (D) Overview, showing the nuclear apparatus and the terminal contractile vacuole. (E, H) Details of anterior body region, showing the oral bulge that is distinctly set off from body proper by the circumoral kinety. Nematodesmata originate from oral dikinetids. (F) Ventral view, showing the curved anterior end of the ciliary rows. (G) Dorsal view of anterior body half, showing the distinctly heterostichad dorsal brush, i.e., the strongly shortened row 3 (arrow). B(1–3), dorsal brush (rows); CK, circumoral kinety; CV, contractile vacuole; E I, type I extrusomes; MA, macronucleus; N, nematodesmata; OB, oral bulge. Scale bars: 2 μm (C), 10 μm (E, F), 20 μm (B, G, H), and 50 μm (D).

Table 1. Morphometric data on *Semispathidium longiarmatum* nov. spec.

Characteristics[a]	Mean	M	SD	SE	CV	Min	Max	*n*
Body, length (μm)	192.4	190.0	29.7	6.8	15.4	142.0	265.0	19
Body, width (μm)	36.2	36.0	4.6	1.1	12.7	29.0	45.0	19
Body, length:width ratio	5.4	5.4	1.0	0.2	19.2	3.6	7.4	19
Oral bulge, length (μm)	11.8	12.0	1.5	0.3	12.4	8.0	14.0	19
Oral bulge, width (μm)	11.4	12.0	1.0	0.2	8.4	10.0	13.0	19
Oral bulge, height (μm)	3.1	3.0	–	–	–	2.5	4.0	19
Anterior body end to macronucleus, distance (μm)	78.3	79.0	19.9	4.6	25.4	40.0	125.0	19
Macronucleus, length (μm)	52.6	52.0	7.0	1.6	13.3	41.0	70.0	19
Macronucleus, width (μm)	10.8	11.0	1.1	0.2	9.8	9.0	14.0	19
Macronucleus, length:width ratio	4.9	4.8	0.6	0.1	11.6	3.9	6.4	19
Macronucleus, number	1.0	1.0	0.0	0.0	0.0	1.0	1.0	19
Micronucleus, length (μm)	3.9	4.0	0.6	0.2	15.5	3.0	5.0	7
Micronucleus, width (μm)	3.3	3.0	0.8	0.3	24.6	2.5	5.0	7
Micronucleus, number	1.0	1.0	0.0	0.0	0.0	1.0	1.0	7
Circumoral kinety to end of brush row 1, distance (μm)	41.2	42.0	7.8	1.8	19.0	29.0	55.0	19
Circumoral kinety to end of brush row 2, distance (μm)	51.4	53.0	10.0	2.3	19.4	33.0	75.0	19
Circumoral kinety to end of brush row 3, distance (μm)	19.9	19.0	4.1	0.9	20.6	14.0	27.0	19
Dikinetids in brush row 1, number	37.5	36.0	8.1	1.8	21.5	24.0	52.0	19
Dikinetids in brush row 2, number	47.3	45.0	9.8	2.2	20.7	33.0	66.0	19
Dikinetids in brush row 3, number	20.0	18.0	4.9	1.1	24.3	15.0	32.0	19
Ciliary rows, number in anterior body third	30.5	30.0	2.6	0.6	8.6	27.0	36.0	19
Ciliated kinetids in a ventral kinety, number	107.7	100.0	22.2	5.1	20.6	75.0	150.0	19
Dorsal brush rows, number	3.0	3.0	0.0	0.0	0.0	3.0	3.0	19
Dorsal brush, % of body length	26.9	26.8	4.5	1.0	16.6	19.2	35.6	19
Dorsal brush rows, maximum length difference (μm)	60.8	60.3	6.2	1.4	10.1	50.9	70.8	19
External oral basket, length (μm)	24.8	25.0	3.6	0.8	14.3	20.0	30.0	19
Cytoplasmic extrusomes, length (μm)	2.4	2.5	–	–	–	2.0	3.0	19
Resting cysts, length in vivo (μm)	60.1	60.0	4.5	1.2	7.5	52.0	70.0	15
Resting cysts, width in vivo (μm)	59.7	60.0	4.3	1.1	7.1	52.0	70.0	15

Abbreviations: CV, coefficient of variation (%); M, median; Max, maximum; Mean, arithmetic mean; Min, minimum; *n*, number of individuals investigated; SD, standard deviation; SE, standard error of arithmetic mean.

[a] Data based, if not stated otherwise, on mounted, protargol-impregnated (Foissner's method), and randomly selected specimens from a non-flooded Petri dish culture.

body axis, shows great flexibility while rooting between soil particles.

Somatic cilia about 10 μm long in vivo; arranged in an average of 30 equidistant, narrowly to ordinarily spaced meridional rows slightly curved anteriorly and abutting on circumoral kinety; basal bodies spaced ordinarily except for about four comparatively densely spaced cilia in curved anterior kinety portion (Figs 1B–D, O, P, 2F, 3A, 4C, D; Table 1). Dorsal brush composed of three rows with ordinarily spaced dikinetids bearing brush bristles up to 3 μm long in vivo; distinctly heterostichad, that is, length difference between shortest and longest row about 60% on average; all rows usually with a short anterior tail of four to six monokinetids with ordinary cilia (Figs 1C, H, O, P, 2C, G, 4A, B, 5A–D; Table 1). Brush row 1 composed of an average of 37 dikinetids: anterior bristle 1.5–2.4 μm long, gradually decreasing posteriorly to 1.0–1.2 μm; posterior bristle stump-like, i.e., only about 1 μm long (SEM observations and measurements); row 1 sometimes shortened anteriorly (Fig. 1C). Brush row 2 longer than row 1 by about 10 μm, composed of an average of 47 dikinetids: anterior and posterior bristle of similar length, i.e., about 1.5–1.8 μm in anterior brush portion, gradually shorten to 0.6–1.1 μm posteriorly in the SEM. Brush row 3 occupies about 40% of length of row 2, composed of an average of 20 dikinetids: anterior bristle about 1.5–2.4 μm long, posterior stump-like and only about 0.9 μm long in the SEM; continues with a long monokinetidal tail extending to or slightly posterior to mid-body with 0.9–1.6 μm long cylindroidal bristles.

Oral bulge occupies slightly to moderately oblique anterior body end (20–45°, mean = 33°, $n = 7$); conspicuous in vivo and in protargol preparations because distinctly set off from body proper and about 5 μm high; discoidal in frontal view with a diameter of 10–14 μm after protargol impregnation and in the SEM; central bulge area concave and dotted by extrusome tips (Figs 1A, B, D, I, J, M–P, 2E, H, 3A, 4C, D; Table 1). Circumoral kinety at base of oral bulge and of same shape, composed of narrowly spaced dikinetids associated with nematodesmata forming an inconspicuous funnel-shaped basket recognizable in some protargol-impregnated specimens (Figs 1B–D, O, P, 2E, F, H, 3A).

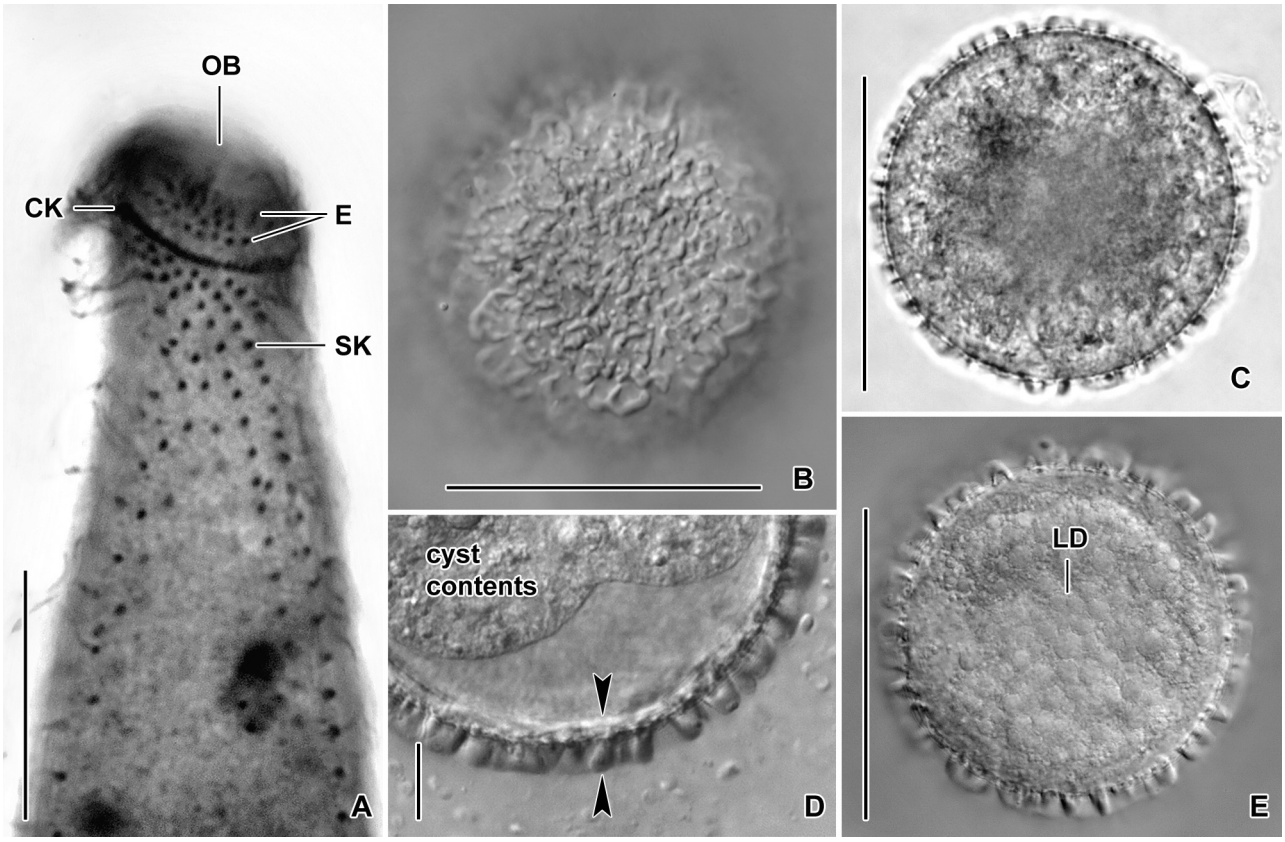

Fig. 3. *Semispathidium longiarmatum* nov. spec. from life (B–E) and after protargol impregnation (A). (A) Detail of anterior body portion, showing the discoidal, inclined oral bulge studded with extrusomes; the continuous dikinetidal circumoral kinety; and the curved anterior end of the somatic kineties. (B) Surface view of a resting cyst, showing the small ribs separated by furrows. (C, E) Resting cysts in bright field and interference contrast. They are about 60 μm in diameter and packed with about 3–4 μm-sized lipid droplets. (D) The cyst wall (opposed arrowheads) is very conspicuous because about 7 μm thick and composed of a 2 μm thick compact internal layer and an about 5 μm thick external layer with small ribs separated by furrows (B). The bands are about 3–5 × 1–4 μm in size and appear as small bridges in optical section through the cyst. CK, circumoral kinety; E, extrusomes; LD, lipid droplets; OB, oral bulge; SK, somatic kinety. Scale bars: 10 μm (A, D) and 50 μm (B, C, E).

Resting cyst: Cysts in vivo colourless, globular to rotund, about 60 μm in diameter; without escape apparatus (Table 1). Cyst wall very conspicuous because about 7 μm thick, i.e., composed of a 2 μm thick, compact internal layer and an about 5 μm thick external layer with wrinkled and irregularly arranged ribs separated by furrows (Figs 1L, 3B); ribs about 3–5 × 1–4 μm in size and appearing as small bridges in optical section (Figs 1K, 3C–E). Cytoplasm packed with 1–5 μm, usually 3–4 μm-sized lipid droplets. Macronucleus slightly shortened, in cyst center, shape unchanged, i.e., narrowly ellipsoidal (Fig. 1K). Contractile vacuole, extrusomes, cortical granules, and cilia not recognizable.

Occurrence: As yet, *S. longiarmatum* has been found only at type locality, i.e., in soil from the Chobe River floodplain in the Chobe National Park, Botswana, tropical Africa. The sampling area was overgrown with grass and is about 25 km west of the town of Kasane, that is, on the so-called Kabolebole Peninsula of the Chobe Riverfront. The sample was collected in February 2001, when the river was almost desiccated. Small amounts of soil and litter from the upper 10-cm layer were collected from the riverbank and from elephant pits in the surroundings. These subsamples were mixed to a composite sample consisting of wet, almost black, rather sandy, and very humic soil.

Multivariate morphometric analyses

Correlation analyses: The first run of correlation analyses revealed several rather highly correlated pairs of morphometric features, reaching values greater than 0.90. However, only two of them, namely, the length of brush row 2 and the number of dikinetids in brush row 2, formed strongly correlated pairs together and with some other features, exceeding the critical value of 0.95. Thus, these two features were excluded from further analyses. A subsequent second run of correlation analyses showed that the length of brush row 3 and the number of dikinetids comprising it, had to be excluded from the multivariate analyses for the same reason. Also other brush features (i.e., length of brush row 1 and number of its

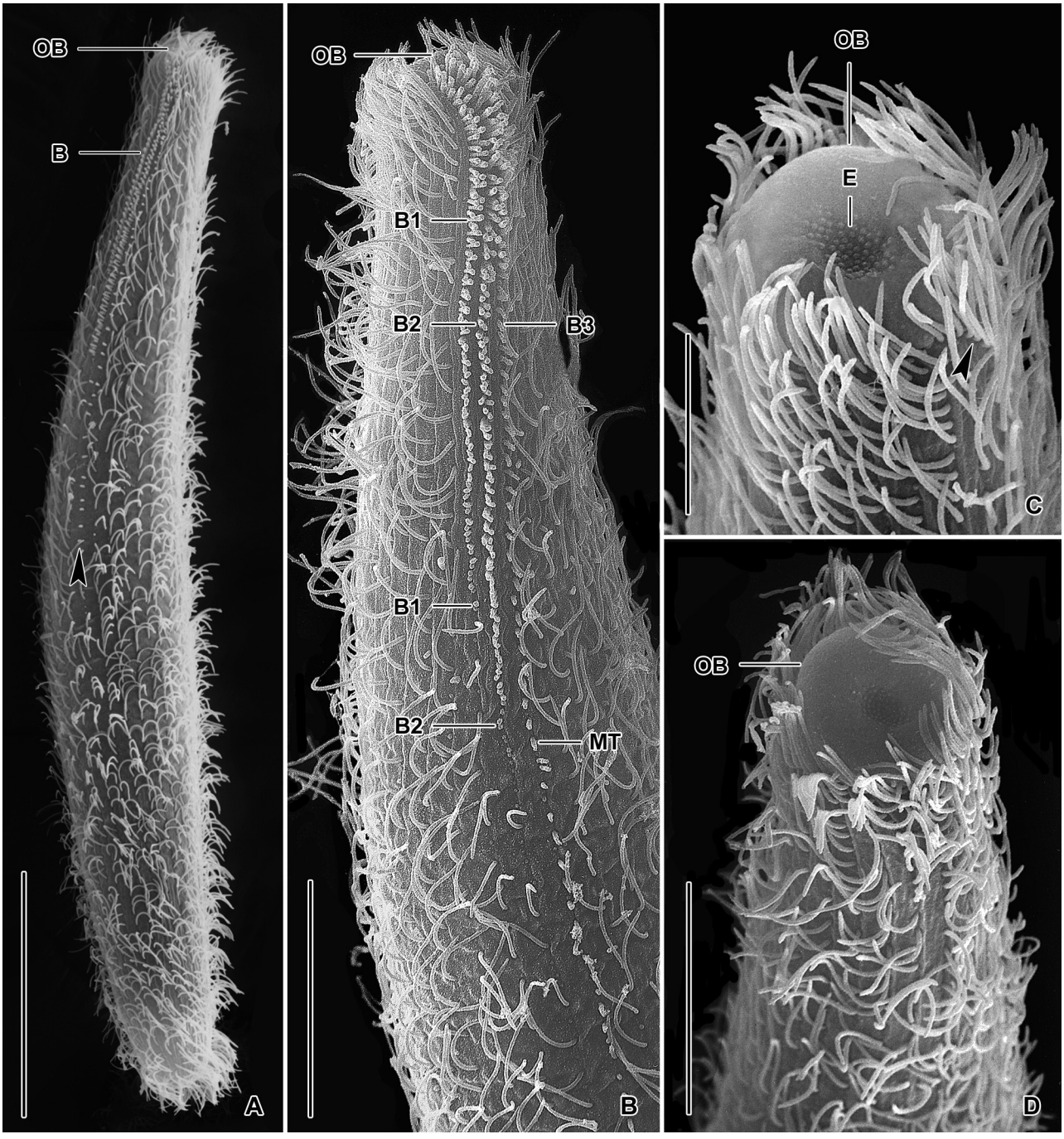

Fig. 4. *Semispathidium longiarmatum* nov. spec. in the scanning electron microscope. (A) Dorsal overview, showing the slender body carrying a three-rowed dorsal brush. The monokinetidal tail of brush row 3 extends to mid-body (arrowhead), as typical for many spathidiids. (B) Detail of anterior body half, showing the distinctly heterostichad dorsal brush (dikinetidal part of brush row 3 > 50% shorter than that of rows 1 and 2) with a long monokinetidal tail extending to mid-body. The end of the dikinetidal part of brush row 3 is marked by "B3"; the same applies to rows 1 and 2. (C, D) The oral bulge is discoidal and has a concave center dotted by extrusome tips. Arrowhead in (C) marks the curved anterior end of a somatic kinety, a diagnostic feature of the genus *Semispathidium*. B(1–3), dorsal brush (rows); E, extrusome tips; MT, monokinetidal tail of brush row 3; OB, oral bulge. Scale bars: 10 μm (C), 20 μm (B, D), and 50 μm (A).

dikinetids as well as the percentage of the longest brush row to body length) were strongly correlated, but they did not exceed the critical value and thus could be assessed by the multivariate analyses. A note regarding the percentage of the longest brush row to body length is needed. In *Semispathidium*, the longest brush row is either row 1 or row 2 (see Table 1 and supplementary Table S1). Calculation of percentage of the longest brush row to body length resulted in a new derived

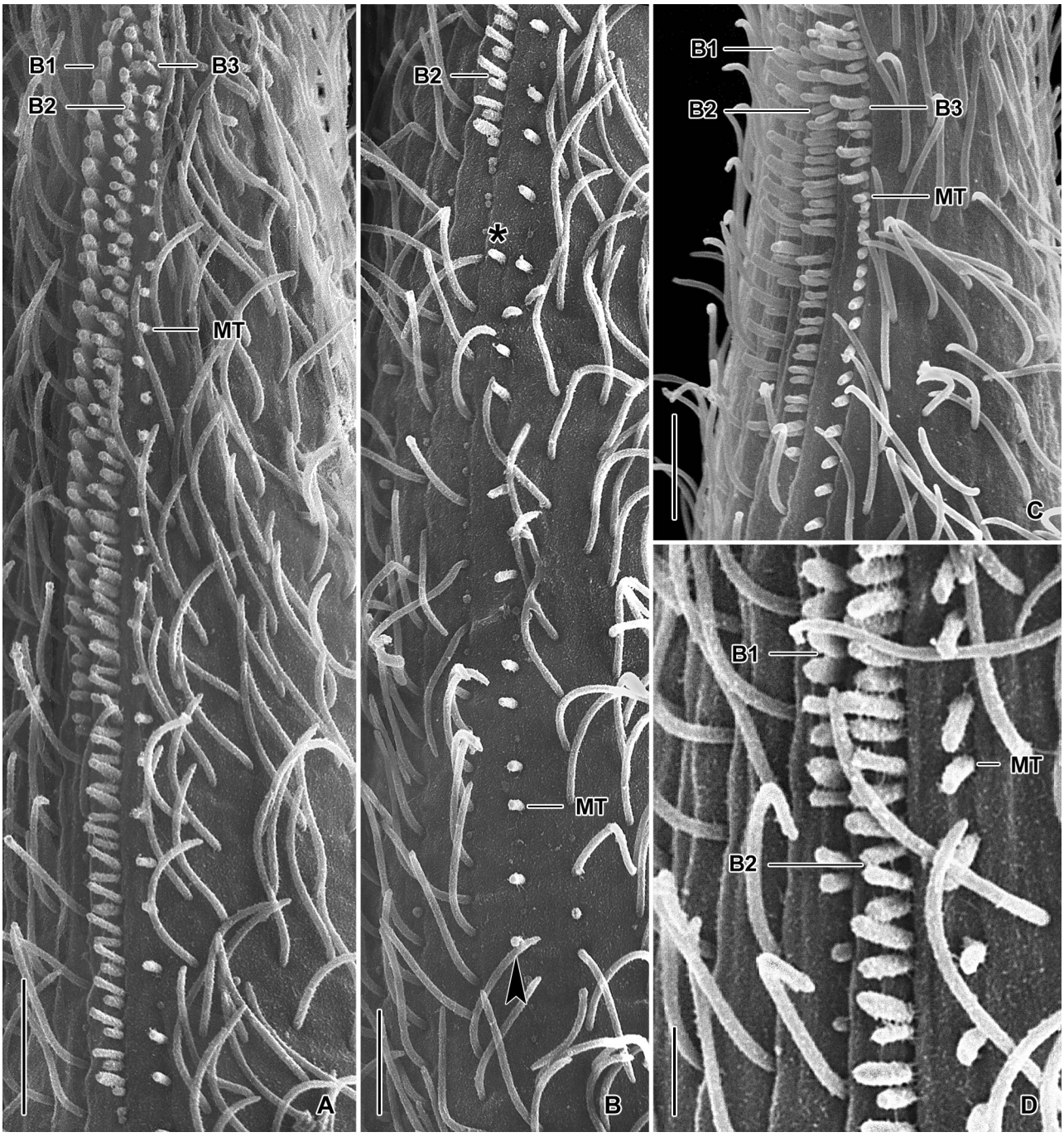

Fig. 5. *Semispathidium longiarmatum* nov. spec., details of the dorsal brush (for overviews, see Fig. 4A, B) in the scanning electron microscope. In most spathidiids, this special structure is composed of three rows with ordinarily spaced dikinetids bearing short bristles, i.e., modified cilia. The dorsal brush of *S. longiarmatum* is distinctly heterostichad, i.e., the length difference between the shortest and the longest row is about 60% on average. Brush row 1 is composed of an average of 37 dikinetids associated with anterior bristles that decrease in length from 1.5–2.4 μm anteriorly to 1–1.2 μm posteriorly; the posterior bristle of the dikinetids is only ~ 1 μm long. Brush row 2 consists of an average of 47 dikinetids bearing bristles of similar length (1.5–1.8 μm) in the distal portion while both or only the posterior bristle decreases to 0.6–1.1 μm in the proximal portion (A, D). Brush row 3 is composed of an average of 20 dikinetids associated with 1.5–2.4 μm long anterior bristles and posterior stumps being only about 0.9 μm long (C). This row continues posteriorly as a monokinetidal tail that extends to or slightly posterior to mid-body with 0.9–1.6 μm long, cylindroidal bristles. The arrowhead in (B) marks the monokinetidal tail of brush row 3; the asterisk denotes an extra tail bristle left of brush row 3. B(1–3), dorsal brush (rows); MT, monokinetidal tail of brush row 3. Scale bars: 2 μm (D) and 5 μm (A–C).

ratio variable that was less strongly correlated than the original variables and thus could be included into multivariate analyses.

Exploratory and cluster analyses: Selected results of exploratory data analyses are shown in Fig. 6. Altogether, we carried out eight cluster analyses. They consistently showed that *S. enchelyodontides* and *S. fraterculum* form very distinct clusters. In contrast, specimens of *S. armatum*, *S. breviarmatum* and *S. longiarmatum* were mixed in a variable pattern that more or less reflected the properties of the clustering algorithm rather than the structure of the data. The UPGMA and centroid methods resulted in dendrograms most consistent with the results obtained with PCA and CDA. Therefore, we present here only the dendrogram generated by the centroid method in a combination with the Manhattan city block as a coefficient of distance (Fig. 7).

Principal component analyses: To get a first insight into the morphometric variation of the five *Semispathidium* species, we performed a PCA on 85 individuals and 16 morphometric features. Three mutually isolated groups of specimens were separated along the first and the second ordination axis of the PCA1 diagram (Fig. 8A). Two groups in the left part of the diagram were clearly homogenous. The first one in the lower left corner can be ascribed to *S. enchelyodontides*. The second group, which was plotted in the upper left corner, was segregated along the second ordination axis and belongs to *S. fraterculum*. The largest group spreading rightwards in the central part of the diagram comprises a mixture of individuals belonging to *S. breviarmatum*, *S. longiarmatum*, and *S. armatum*. However, specimens of *S. breviarmatum* showed a trend to separate from *S. longiarmatum* and *S. armatum* along the first axis (Fig. 8A). The following morphometric features most contributed to the distinction of the three main groups along the first ordination axis: (i) length of brush row 1, (ii) number of dikinetids in brush row 1, (iii) width of macronucleus, and (iv) number of ciliated kinetids in a ventral kinety. The second ordination axis reached highest correlations with the (i) length of macronucleus, (ii) length/width ratio of macronucleus, (iii) number of macronuclear nodules, and (iv) height of oral bulge (Table 2).

The second set of PCA was based on a reduced dataset with 15 features and 46 individuals of three closely related taxa, viz., *S. breviarmatum*, *S. longiarmatum*, and *S. armatum*. PCA2 reached only a slightly higher differentiation among these three species than PCA1 did. Although individuals belonging to *S. breviarmatum* formed an essentially independent group, the two other taxa remained together (Fig. 8B). The strongest influence on the separation along the first axis possessed the following features: (i) length of brush row 1, (ii) number of dikinetids in brush row 1, (iii) length of oral bulge, (iv) height of oral bulge, and (v) width of macronucleus (Table 2).

Canonical discriminant analyses: These were used to test whether populations from different collection sites can be distinguished by the quantitative features measured and scored. In contrast to the foregoing PCA1 and PCA2, the CDA1 (85 individuals and 15 morphometric features) displayed the five *Semispathidium* taxa essentially separated along the first three canonical axes (Fig. 8C). Numerous morphometric features correlated highly with the first canonical axis but the most substantial contribution can be attributed to the (i) number of ciliary rows, (ii) number of dikinetids in brush row 1, (iii) width of macronucleus, (iv) length of brush row 1, (v) number of ciliated kinetids in a ventral kinety, and (vi) percentage of longest dorsal brush row to body length. The length/width ratio of the macronucleus and the length of the macronucleus (nodule) correlated best with canonical axis 2, and the height of the oral bulge correlated best with the third axis (Table 2).

As *S. longiarmatum* and *S. armatum* could not be clearly separated by the foregoing analyses, we subjected them to two further canonical discriminant analyses. The CDA2A comprised 27 individuals and 15 morphometric features. A clear separation without any overlap was apparent (Fig. 8D). This strong separation was, however, significantly influenced by only a single feature, viz., the number of ciliary rows. Therefore, we searched for other features that might distinguish these taxa by generating a new dataset, CDA2B, in which we excluded the number of ciliary rows (27 individuals and 14 morphometric features). The CDA2B repeatedly showed a clear separation of both taxa by the length/width ratio of the macronucleus and by the number of dikinetids in brush row 1 (Fig. 8E; Table 2).

Discussion

Comparison of the new species with the congeners

Among the congeners, *S. longiarmatum* nov. spec. is most similar to *S. armatum* and *S. breviarmatum*. They can be separated from each other by the shape and pattern of the extrusomes. *Semispathidium longiarmatum* exhibits two shape and size types of oral extrusomes: type I is very narrowly cuneate and 9–11 μm long and type II is oblong and only about 2 μm long. *Semispathidium armatum* and *S. breviarmatum* display only one type of oral extrusomes, obclavate with a rod-shaped anterior process in the former, and narrowly ovate and only 5–7 μm long in the latter. Morphometrically, *S. longiarmatum* is separated from *S. armatum* by the higher number of ciliary rows (27–36 vs. 20–23), and from *S. breviarmatum* by the much lower number of dikinetids in brush row 1 (24–52 vs. 52–102).

Semispathidium longiarmatum resembles *S. lagyniforme*, as redescribed by Foissner (1984), in the macronuclear pattern but differs by the larger body (165–300 μm vs. 100–160 μm) and the shape and size of the extrusomes (very narrowly cuneate and 9–11 μm long vs. oblong to bluntly fusiform and about 5 μm long). Finally, *S. longiarmatum*

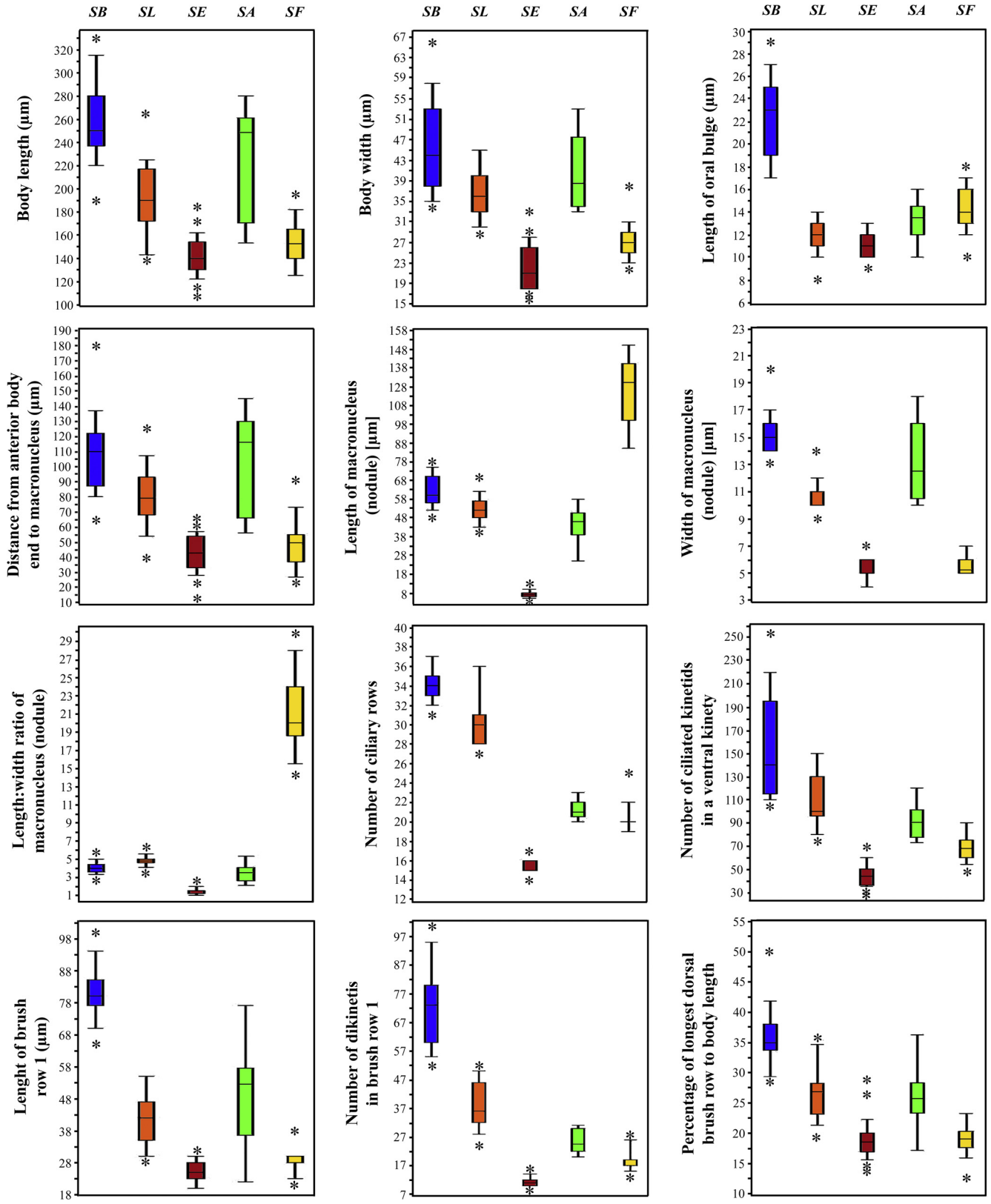

Fig. 6. Box-plot graphs showing variation of 12 selected morphometric features of five *Semispathidium* species. Rectangles represent the 25th and 75th percentiles; horizontal lines show the median; whiskers are from the 10th to the 90th percentiles; asterisks denote extreme values. SA, *S. armatum* (green colour); SB, *S. breviarmatum* (blue colour); SE, *S. enchelyodontides* (red colour); SF, *S. fraterculum* (yellow colour); SL, *S. longiarmatum* (orange colour). (For interpretation of the references to colour in this figure legend, the reader is referred to the web version of this article.)

Table 2. Numerical output of the multivariate analyses.

Characteristics	PCA1[a]		PCA2[a]		CDA1[a]			CDA2A[a]	CDA2B[a]
	Axis 1	Axis 2	Axis 1	Axis 2	Axis 1	Axis 2	Axis 3	Axis 1	Axis 1
Body length (μm)	0.294779	−0.063572	0.288989	0.347570	0.789466	−0.126417	0.138214	−0.385717	−0.403372
Body width (μm)	0.296843	0.033357	0.258323	−0.205405	0.794847	−0.058724	−0.021467	−0.366310	−0.383076
Body length:width ratio	−0.070936	−0.169470	0.060617	0.517008	−0.216864	−0.151480	0.259992	−0.072505	−0.075824
Length of oral bulge (μm)	0.259612	0.137241	**0.325937**	−0.017805	0.719130	0.181197	0.551997	−0.393015	−0.411004
Height of oral bulge (μm)	0.053214	**0.325142**	**0.305812**	−0.022274	0.133602	0.513679	**0.673938**	−0.420347	−0.439587
Distance from anterior body end to macronucleus (μm)	0.279981	−0.087805	0.235768	0.456720	0.727982	−0.139106	0.027469	−0.433040	−0.452861
Length of macronucleus (μm)	0.064076	**0.565182**	0.251134	−0.210408	0.219516	**0.945633**	−0.081822	0.449903	0.470496
Width of macronucleus (μm)	**0.314508**	−0.093484	**0.303966**	0.100075	**0.887187**	−0.226626	0.021942	−0.535030	−0.559519
Length:width ratio of macronucleus	−0.071244	**0.564936**	−0.076932	−0.274078	−0.174509	**0.966155**	−0.048591	0.684281	**0.715602**
Number of macronuclear nodules	−0.212054	**−0.338841**	–	–	–	–	–	–	–
Number of ciliary rows	0.295500	0.033153	0.206776	−0.260355	**0.970188**	0.024462	−0.183342	**0.904555**	–
Number of ciliated kinetids in a ventral kinety	**0.302227**	0.038550	0.277050	−0.165553	**0.863455**	−0.006749	0.035956	0.357785	0.374161
Length of brush row 1 (μm)	**0.315812**	−0.043335	**0.341685**	0.055389	**0.881413**	−0.119745	0.328061	−0.308602	−0.322728
Number of dikinetids in brush row 1	**0.315298**	0.009174	**0.327805**	−0.156671	**0.939072**	−0.039945	0.220368	0.631566	**0.660474**
Percentage of longest dorsal brush row to body length	0.286143	−0.070770	0.255101	−0.266369	**0.838579**	−0.175310	0.126205	0.091488	0.095676
Maximum length difference between the shortest and longest dorsal brush row	0.242045	−0.249345	0.143391	0.192711	0.654393	−0.399558	−0.140245	−0.089644	−0.093747

Abbreviations: See Material and Methods.

[a]Eigenvectors expressing correlations of morphometric features with the principal component axes 1 and 2 (PCA1 and PCA2) and the canonical axes 1–3 (CDA1, CDA2A, and CDA2B). Numbers in bold face mark features strongly correlated with the ordination axes.

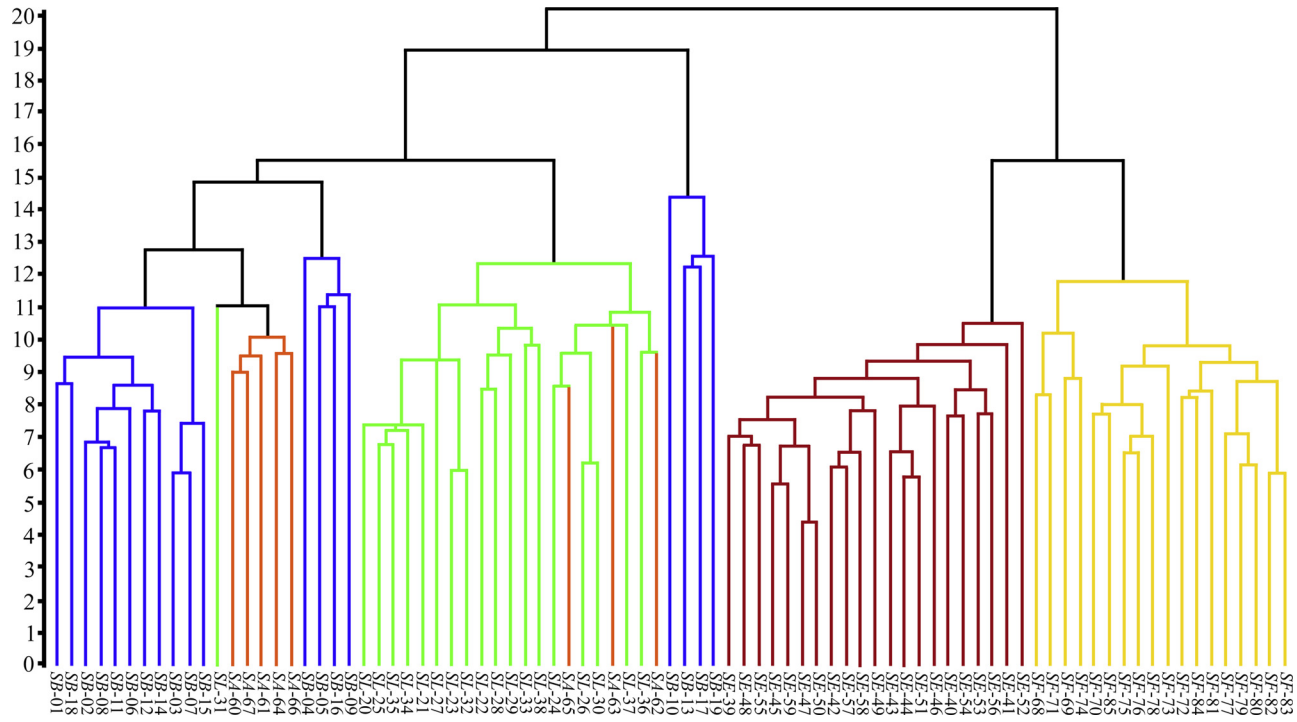

Fig. 7. Cluster analysis (centroid method in combination with the Manhattan city block distance) of 85 specimens of five *Semispathidium* species based on 16 morphometric features. Colour coding of specimens is as follows: *S. armatum*, SA-60–SA-67 (orange); *S. breviarmatum*, SB-01–SB-19 (blue); *S. enchelyodontides*, SE-39–SE-59 (red); *S. fraterculum*, SF-68–SF-85 (yellow); *S. longiarmatum*, SL-20–SL-38 (green). (For interpretation of the references to colour in this figure legend, the reader is referred to the web version of this article.)

is distinguished from the three remaining congeners by the macronuclear pattern. Specifically, the macronucleus is elongate ellipsoidal in *S. longiarmatum* while it is fragmented into about 21 nodules in *S. enchelyodontides* (Foissner et al. 2002) and is a nodulated, tortuous strand in *S. fraterculum* and *S. pulchrum* (Foissner et al. 2010). Moreover, *S. longiarmatum* differs from these species by the shape of the type I extrusomes: filiform in *S. enchelyodontides* and *S. fraterculum*, and very narrowly fusiform in *S. pulchrum*.

Multivariate morphometric methods in alpha-taxonomy

Species recognition is the most essential taxonomic task, especially, nowadays when dozens of new ciliate taxa are described every year. Despite the implementation of molecular techniques, species continue to be delimited with morphological features, both qualitative and quantitative. The reliability of quantitative features can be assessed by a multivariate approach, using cluster, principal component, and canonical discriminant analyses (for review, see Marhold 2011). As these methods have been comparatively rarely applied in ciliate species discrimination (e.g., Berger and Hatzidimitriou 1978; Jones and Gates 1994; Lynn and Malcolm 1983), we provide below their brief description, show their advantages/disadvantages, and discuss data requirements for these techniques to be statistically meaningful.

Cluster analysis is a hierarchical agglomerative method that arranges operational taxonomic units into clusters in a stepwise fashion. The main goal of this statistical technique is grouping of related individuals in such a way that specimens in the same cluster are more similar to each other than to those in other clusters (Everitt 1986; Podani 2001). Cluster analysis is not one specific algorithm, but includes various algorithms that differ in procedure how clusters are constituted. The appropriate clustering algorithm and coefficient of distance depend on individual datasets. Therefore, cluster analysis is not an automatic task, but iterative process involving trial and failure (Marhold 2011; Podani 2001). In the present study, the UPGMA and centroid clustering algorithms in combination with either Euclidean or Manhattan city block distance generated dendrograms most consistent with the results obtained with principal component and canonical discriminant analyses (cp. Fig. 6 with Figs 7, 8). However, also other combinations of clustering algorithms and coefficient of distance may be more appropriate for other ciliate groups or datasets. There are no statistical restrictions concerning the number of analyzed specimens in cluster analysis (Podani 2001).

Principal component analysis (PCA) converts a set of possibly correlated morphometric variables into a set of linearly uncorrelated variables called principal components. The first principal component has the largest possible variance, that

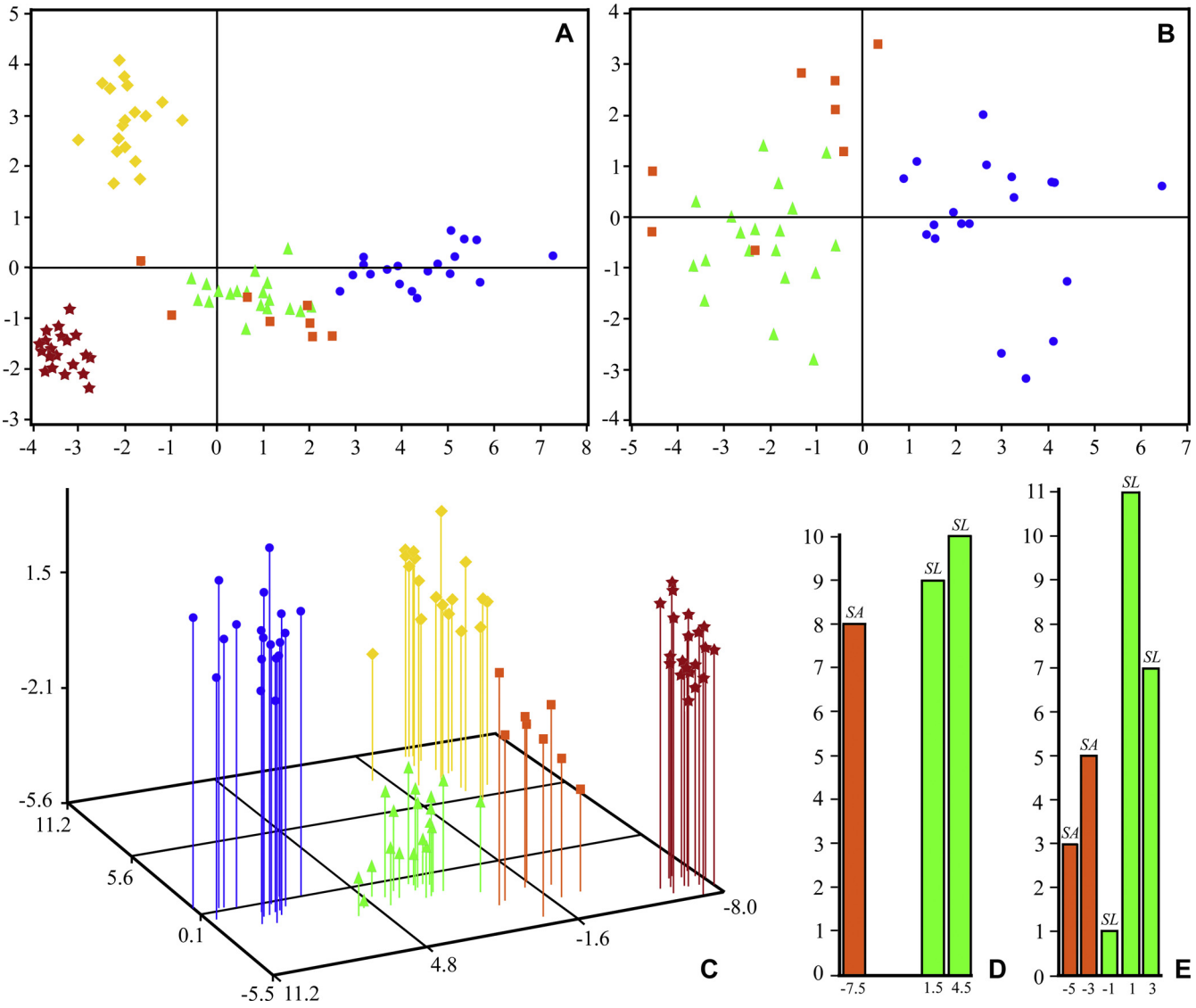

Fig. 8. Multivariate analyses of five African *Semispathidium* species. (A) Principal component analysis (PCA1) of 85 individuals based on 16 morphometric features. Eigenvalues of the two first ordination axes are $\lambda_1 = 0.561$ and $\lambda_2 = 0.175$, explaining 73.6% of the total variation. (B) Principal component analysis (PCA2) of 46 individuals based on 15 morphometric features [number of macronuclear nodules excluded because of its uniformity across the dataset]. Eigenvalues of the two first ordination axes are $\lambda_1 = 0.508$ and $\lambda_2 = 0.139$, explaining 64.7% of the total variation. (C) Canonical discriminant analysis (CDA1) of 85 individuals based on 15 morphometric features [number of macronuclear nodules excluded because of its uniformity in one group]. Eigenvalues of the three first ordination axes are $\lambda_1 = 0.568$, $\lambda_2 = 0.324$ and $\lambda_3 = 0.075$, explaining 96.7% of the total variation. (D) Histogram of canonical discriminant analysis (CDA2A) of *S. armatum* ($n = 8$) and *S. longiarmatum* ($n = 19$) based on 15 morphometric features [number of macronuclei excluded because of its similarity in both species]. (E) Histogram of canonical discriminant analysis (CDA2B) of *S. armatum* ($n = 8$) and *S. longiarmatum* ($n = 19$) based on 14 morphometric features [number of ciliary rows excluded to find out whether there are further features distinguishing these two species]. Code: *S. armatum* (*SA*), orange square; *S. breviarmatum*, blue circle; *S. enchelyodontides*, red asterisk; *S. fraterculum*, yellow rhombus; and *S. longiarmatum* (*SL*), green triangle. (For interpretation of the references to colour in this figure legend, the reader is referred to the web version of this article.)

is, accounts for as much of the variability in the dataset as possible. Each succeeding component has the highest variance possible under the constraint that it is uncorrelated with the preceding component(s), whereby the eigenvalues represent the variance extracted by each principal component. In this way, PCA brings insight into the overall variation of the dataset and expresses relationships between specimens and their morphometric characters that are extracted along the ordination axes, i.e., principal components (Krzanowski 1990; Marhold 2011; Sneath and Sokal 1973). The minimum number of specimens required for this method is at least by one greater than the number of used morphometric characters. However, it is recommended that the number of specimens should be approximately the square number of morphometric characters (Legendre and Legendre 1998).

Canonical discriminant analysis is an ordination method used to reveal the extent of morphological differentiation between predefined groups that were proposed either by cluster analysis, PCA or on the basis of genetic, geographic or ecological differences. In this technique, canonical discriminant functions (axes) are derived from a linear combination of the original morphometric characters. However, unlike in PCA, the characters are weighted to maximize differences among tested groups. Correlation of the original characters with canonical axes, i.e., the contribution of individual characters to group separation are expressed by values of the total canonical structure (Klecka 1980; Krzanowski 1990). Requirements for data in CDA include: (i) objects should be characterized by quantitative and/or binary characters; (ii) no character can be a linear combination of any other characters; (iii) any pair of characters cannot be highly correlated ($r > 0.95$); (iv) covariance matrices should be approximately equal; (v) the distribution of characters within each group should be multivariate normal; (vi) no character can be invariant in any predefined group; and (vii) for the number of groups (g), characters (p) and total number of objects (n) should hold: $0 < p < (n - g)$; however, in general, the number of objects (specimens) should be significantly higher than the number of morphometric characters (Marhold 2011).

Morphometric taxonomy of *Semispathidium*

In the present study, we analyzed species boundaries and evaluated the importance of various morphometric features for species identification in the genus *Semispathidium*. Principal component and canonical discriminant analyses showed that the majority of morphometric features reliably separate the five *Semispathidium* species analyzed (Fig. 8 and Table 2). The most substantial contribution can be attributed to the (i) macronuclear pattern, i.e., length and width of macronucleus as well as the number of macronuclear nodules; (ii) number of ciliary rows and of ciliated kinetids in a ventral kinety; (iii) length of brush row 1 and the number of dikinetids in that row; and (iv) to the percentage of the longest dorsal brush row to body length. Body length and width as well as the distance from the anterior body end to the beginning of the macronucleus are comparatively poorly correlated with the ordination axes (Table 2), and thus only slightly contribute to species delimitation. This is due to their high variability, causing significant transitions (Fig. 6). Nevertheless, body size is one of the most important features of a ciliate species and can be used for keying out many spathidiid species (Foissner and Xu 2007). For instance, although *S. longiarmatum* cannot be separated from *S. armatum* and *S. breviarmatum* by body size, this feature clearly distinguishes it from *S. lagyniforme*. The separation of *S. longiarmatum* from *S. lagyniforme* is corroborated also by at least one qualitative feature, viz., the shape of the extrusomes (see above). Since these organelles are used for capturing and killing the prey, they are biologically important for survival and hence are also taxonomically indispensable in predatory ciliates (e.g., Foissner and Xu 2007, Foissner et al. 2002, 2010; Vďačný and Foissner 2012, 2013).

Morphology of the dorsal brush, a special field of sensoric cilia typically localized in the anterior region of some dorsal and/or left lateral ciliary rows, is taxonomically very important in free-living litostomateans (Foissner and Xu 2007; Vďačný and Foissner 2012). However, this could be only partially tested in the present study because half of brush features had to be excluded from PCA and CDA, as they formed critically correlated ($r > 0.95$) pairs that distort this type of statistical techniques (Legendre and Legendre 1998; Marhold 2011). Finally, only four brush features could be subjected to multivariate analyses because their correlation coefficients did not exceed the critical value of 0.95, although they formed strongly correlated pairs ($r > 0.90$). These included: (i) length of brush row 1; (ii) number of dikinetids in that row; (iii) percentage of the longest dorsal brush row to body length; and (iv) maximum length difference between the shortest and longest dorsal brush row. The present multivariate analyses showed that the former three brush features significantly contributed to separation of *Semispathidium* species (Table 2). Thus, quantitative brush features might be considered reliable markers for recognition of spathidiid ciliates in particular and free-living litostomateans in general.

Like in *Semispathidium*, multivariate statistical analyses carried out on colpodids showed that some morphological characters, which were traditionally considered important by taxonomists, clearly separate *Colpoda* species (Foissner and Schubert 1983; Lynn and Malcolm 1983). As in *Semispathidium*, several key morphometric features were strongly correlated in 21 different isolates of the *Euplotes charon* morphotype (Jones and Gates 1994). Further, principal component analysis revealed continua in these characters among the *E. charon*-like strains, causing the traditional criteria used for species separation within this morphotype to be insufficient. Three *Semispathidium* species also formed a continuum in the principal component analyses (Fig. 8A, B), but these three taxa were clearly differentiated by the canonical discriminant analyses (Fig. 8C–E). This indicates the latter statistical technique to be a more powerful tool for species discrimination than principal component analysis.

To summarize, our study demonstrates the reliability of the five analyzed *Semispathidium* species. This is corroborated not only by qualitative features such as the extrusome and macronuclear pattern but also, independently, by quantitative (morphometric) features. Consequently, *Semispathidium* species do not form a continuous complex but, rather, fairly discrete clusters in the phenotypic space. Since *Semispathidium* very likely evolved and radiated in central and southern Africa, our analysis shows that raptorial ciliates can form distinct groups also in sympatry.

Acknowledgements

We are grateful to Dr. Helmut Berger and two anonymous reviewers for their thoughtful comments that led to

improvements in the manuscript. Financial support was provided by the Austrian Science Fund (FWF project P-19699-B17 and P-22846-B17 to Wilhelm Foissner) and the Slovak Scientific Grant Agency (VEGA project 1/0248/13 to Peter Vďačný). This work was supported also by the Slovak Research and Development Agency under the contract No. APVV-0436-12. The technical assistance of Mag. Barbara Harl and Robert Schörghofer is greatly appreciated.

References

Berger, J., Hatzidimitriou, G., 1978. Multivariate morphometric analyses of demic variation in *Ancistrum mytili* (Ciliophora: Scuticociliatida) commensal in two mytilid pelecypods. Protistologica 14, 133–153.

Everitt, B., 1986. Cluster Analysis, 2nd ed. Halsted Press, New York.

Foissner, W., 1984. Infraciliatur, Silberliniensystem und Biometrie einiger neuer und wenig bekannter terrestrischer, limnischer und mariner Ciliaten (Protozoa: Ciliophora) aus den Klassen Kinetofragminophora, Colpodea und Polyhymenophora. Stapfia 12, 1–165.

Foissner, W., 1991. Basic light and scanning electron microscopic methods for taxonomic studies of ciliated protozoa. Eur. J. Protistol. 27, 313–330.

Foissner, W., 1998. An updated compilation of world soil ciliates (Protozoa, Ciliophora), with ecological notes, new records, and descriptions of new species. Eur. J. Protistol. 34, 195–235.

Foissner, W., Schubert, G., 1983. Morphologische und diskriminanzanalytische Trennung von *Colpoda aspera* Kahl, 1926 und *Colpoda elliotti* Bradbury et Outka, 1967 (Ciliophora: Colpodidae). Acta Protozool. 22, 127–138.

Foissner, W., Xu, K., 2007. Monograph of the Spathidiida (Ciliophora, Haptoria). Vol. I: Protospathidiidae, Arcuospathidiidae, Apertospathulidae. Springer-Verlag, Dordrecht.

Foissner, W., Berger, H., Blatterer, H., Kohmann, F., 1995. Taxonomische und ökologische Revision der Ciliaten des Saprobiensystems - Band IV: Gymnostomatea, *Loxodes*, Suctoria. Informationsberichte des Bayer. Landesamtes für Wasserwirtschaft 1/95, 1–540.

Foissner, W., Agatha, S., Berger, H., 2002. Soil ciliates (Protozoa, Ciliophora) from Namibia (Southwest Africa) with emphasis on two contrasting environments, the Etosha region and the Namib Desert. Denisia 5, 1–1459.

Foissner, W., Hess, S., Al-Rasheid, K., 2010. Two vicariant *Semispathidium* species from tropical Africa and central Europe: *S. fraterculum* nov. spec. and *S. pulchrum* nov. spec. (Ciliophora, Haptorida). Eur. J. Protistol. 46, 61–73.

Ginoris, Y.P., Amaral, A.L., Nicolau, A., Coelho, M.A.Z., Ferreira, E.C., 2007. Raw data pre-processing in the protozoa and metazoa identification by image analysis and multivariate statistic techniques. J. Chemometrics 21, 156–164.

Jones, T.C., Gates, M.A., 1994. A morphometric analysis of the *Euplotes charon* morphotype (Ciliophora: Euplotida). J. Eukaryot. Microbiol. 41, 441–450.

Kahl, A., 1930. Urtiere oder Protozoa I: Wimpertiere oder Ciliata (Infusoria) 1. Allgemeiner Teil und Prostomata. Tierwelt Dtl. 18, 1–180.

Klecka, W.R., 1980. Discriminant Analysis. Sage Publications, Beverly Hills/London.

Krzanowski, W.J., 1990. Principles of Multivariate Analysis. Clarendon Press, Oxford.

Legendre, P., Legendre, L., 1998. Numerical Ecology, 2nd ed. Elsevier, Amsterdam.

Lin, X., Warren, A., Song, W., 2009. Pleurostomatids. In: Song, W., Warren, A., Hu, X. (Eds.), Free-Living Ciliates in the Bohai and Yellow Seas. Science Press, Beijing, pp. 93–134.

Lynn, D.H., 2008. The Ciliated Protozoa. Characterization, Classification, and Guide to the Literature, 3rd ed. Springer, Dordrecht.

Lynn, D.H., Malcolm, J.R., 1983. A multivariate study of morphometric variation in species of the ciliate genus *Colpoda* (Ciliophora: Colpodida). Can. J. Zool. 61, 307–316.

Marhold, K., 2011. Multivariate morphometrics and its application to monography at specific and infraspecific levels. In: Stuessy, T.F., Lack, H.W. (Eds.), Monographic Plant Systematics: Fundamental Assessment of Plant Biodiversity. Gantner Verlag, Ruggell, pp. 73–99.

Podani, J., 2001. SYN-TAX. Version 5.0. Computer Programs for Multivariate Data Analysis in Ecology and Systematics. User's Guide. Scientia Publishing, Budapest.

Rosati, G., Modeo, L., 2003. Extrusomes in ciliates: diversification, distribution, and phylogenetic implications. J. Eukaryot. Microbiol. 50, 383–402.

SAS INSTITUTE, 2000. SAS OnlineDoc®, version 8. SAS Institute, Cary.

Sneath, P.H.A., Sokal, R.R., 1973. Numerical Taxonomy. The Principles and Practice of Numerical Classification. Freeman and Company, San Francisco.

Vďačný, P., Foissner, W., 2012. Monograph of the dileptids (Protista, Ciliophora, Rhynchostomatia). Denisia 31, 1–529.

Vďačný, P., Foissner, W., 2013. Synergistic effects of combining morphological and molecular data in resolving the phylogenetic position of *Semispathidium* (Ciliophora, Haptoria), with description of *S. breviarmatum* sp. n. from tropical Africa. Zool. Scr. 42, 529–549.